63

SATELLITE & MESOMETEOROLOGY RESEARCH PROJECT

Department of the Geophysical Sciences
The University of Chicago

PRELIMINARY INVESTIGATION OF PERIPHERAL SUBSIDENCE ASSOCIATED WITH HURRICANE OUTFLOW

by

Ronald M. Reap

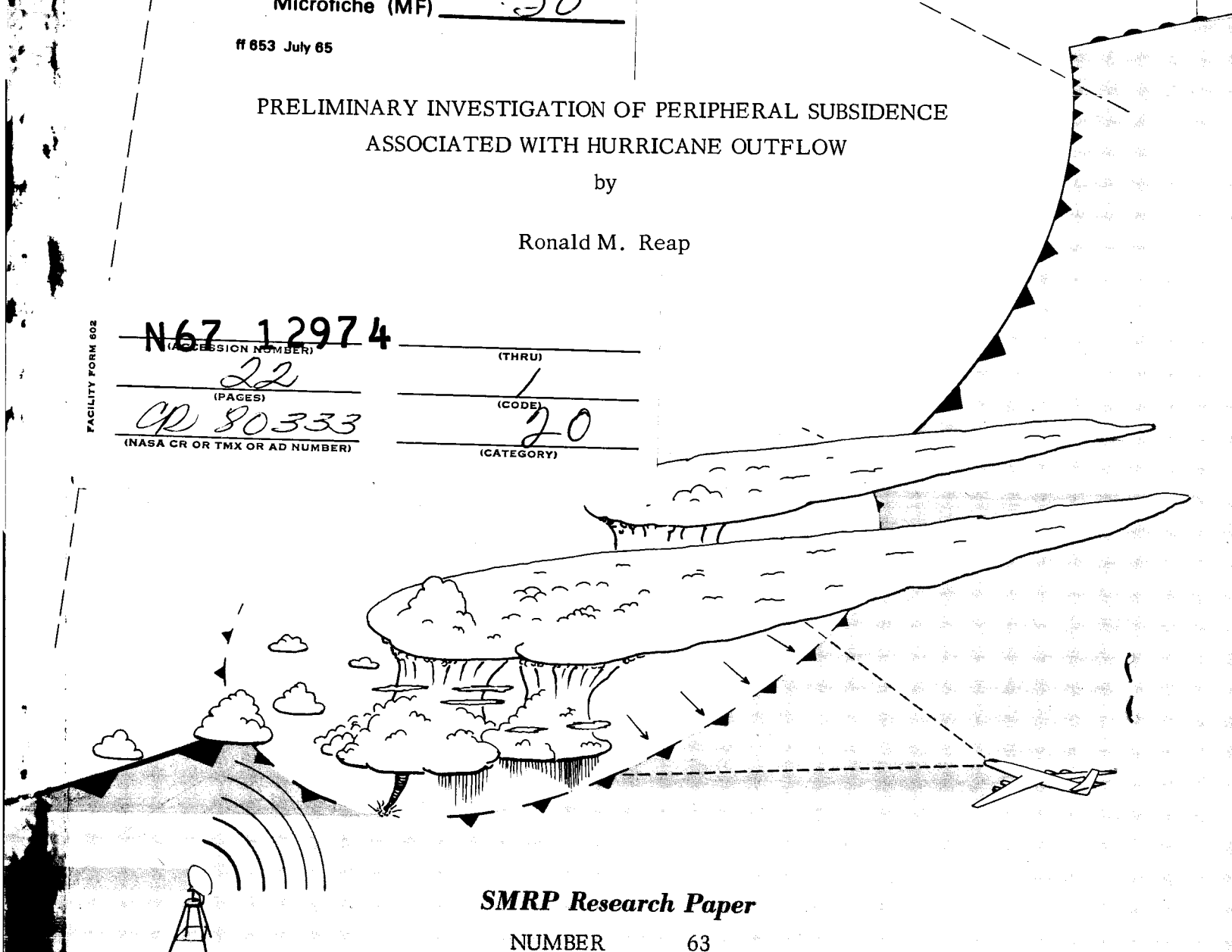

SMRP Research Paper

NUMBER 63

July 1966

MESOMETEOROLOGY PROJECT --- RESEARCH PAPERS

1.* Report on the Chicago Tornado of March 4, 1961 - Rodger A. Brown and Tetsuya Fujita

2.* Index to the NSSP Surface Network - Tetsuya Fujita

3.* Outline of a Technique for Precise Rectification of Satellite Cloud Photographs - Tetsuya Fujita

4.* Horizontal Structure of Mountain Winds - Henry A. Brown

5.* An Investigation of Developmental Processes of the Wake Depression Through Excess Pressure Analysis of Nocturnal Showers - Joseph L. Goldman

6.* Precipitation in the 1960 Flagstaff Mesometeorological Network - Kenneth A. Styber

7.** On a Method of Single- and Dual-Image Photogrammetry of Panoramic Aerial Photographs - Tetsuya Fujita

8. A Review of Researches on Analytical Mesometeorology - Tetsuya Fujita

9. Meteorological Interpretations of Convective Nephsystems Appearing in TIROS Cloud Photographs - Tetsuya Fujita, Toshimitsu Ushijima, William A. Hass, and George T. Dellert, Jr.

10. Study of the Development of Prefrontal Squall-Systems Using NSSP Network Data - Joseph L. Goldman

11. Analysis of Selected Aircraft Data from NSSP Operation, 1962 - Tetsuya Fujita

12. Study of a Long Condensation Trail Photographed by TIROS I - Toshimitsu Ushijima

13. A Technique for Precise Analysis of Satellite Data; Volume I - Photogrammetry (Published as MSL Report No. 14) - Tetsuya Fujita

14. Investigation of a Summer Jet Stream Using TIROS and Aerological Data - Kozo Ninomiya

15. Outline of a Theory and Examples for Precise Analysis of Satellite Radiation Data - Tetsuya Fujita

16. Preliminary Result of Analysis of the Cumulonimbus Cloud of April 21, 1961 - Tetsuya Fujita and James Arnold

17. A Technique for Precise Analysis of Satellite Photographs - Tetsuya Fujita

18. Evaluation of Limb Darkening from TIROS III Radiation Data - S.H.H. Larsen, Tetsuya Fujita, and W.L. Fletcher

19. Synoptic Interpretation of TIROS III Measurements of Infrared Radiation - Finn Pedersen and Tetsuya Fujita

20. TIROS III Measurements of Terrestrial Radiation and Reflected and Scattered Solar Radiation - S.H.H. Larsen, Tetsuya Fujita, and W.L. Fletcher

21. On the Low-level Structure of a Squall Line - Henry A. Brown

22. Thunderstorms and the Low-level Jet - William D. Bonner

23. The Mesoanalysis of an Organized Convective System - Henry A. Brown

24. Preliminary Radar and Photogrammetric Study of the Illinois Tornadoes of April 17 and 22, 1963 - Joseph L. Goldman and Tetsuya Fujita

25. Use of TIROS Pictures for Studies of the Internal Structure of Tropical Storms - Tetsuya Fujita with Rectified Pictures from TIROS I Orbit 125, R/O 128 - Toshimitsu Ushijima

26. An Experiment in the Determination of Geostrophic and Isallobaric Winds from NSSP Pressure Data - William Bonner

27. Proposed Mechanism of Hook Echo Formation - Tetsuya Fujita with a Preliminary Mesosynoptic Analysis of Tornado Cyclone Case of May 26, 1963 - Tetsuya Fujita and Robbi Stuhmer

28. The Decaying Stage of Hurricane Anna of July 1961 as Portrayed by TIROS Cloud Photographs and Infrared Radiation from the Top of the Storm - Tetsuya Fujita and James Arnold

29. A Technique for Precise Analysis of Satellite Data, Volume II - Radiation Analysis, Section 6. Fixed-Position Scanning - Tetsuya Fujita

30. Evaluation of Errors in the Graphical Rectification of Satellite Photographs - Tetsuya Fujita

31. Tables of Scan Nadir and Horizontal Angles - William D. Bonner

32. A Simplified Grid Technique for Determining Scan Lines Generated by the TIROS Scanning Radiometer - James E. Arnold

33. A Study of Cumulus Clouds over the Flagstaff Research Network with the Use of U-2 Photographs - Dorothy L. Bradbury and Tetsuya Fujita

34. The Scanning Printer and Its Application to Detailed Analysis of Satellite Radiation Data - Tetsuya Fujita

35. Synoptic Study of Cold Air Outbreak over the Mediterranean using Satellite Photographs and Radiation Data - Aasmund Rabbe and Tetsuya Fujita

36. Accurate Calibration of Doppler Winds for their use in the Computation of Mesoscale Wind Fields - Tetsuya Fujita

37. Proposed Operation of Intrumented Aircraft for Research on Moisture Fronts and Wake Depressions - Tetsuya Fujita and Dorothy L. Bradbury

38. Statistical and Kinematical Properties of the Low-level Jet Stream - William D. Bonner

39. The Illinois Tornadoes of 17 and 22 April 1963 - Joseph L. Goldman

40. Resolution of the Nimbus High Resolution Infrared Radiometer - Tetsuya Fujita and William R. Bandeen

41. On the Determination of the Exchange Coefficients in Convective Clouds - Rodger A. Brown

* Out of Print
** To be published

(Continued on back cover)

SATELLITE AND MESOMETEOROLOGY RESEARCH PROJECT
Department of the Geophysical Sciences
The University of Chicago

PRELIMINARY INVESTIGATION OF PERIPHERAL SUBSIDENCE ASSOCIATED WITH HURRICANE OUTFLOW

by

Ronald M. Reap

SMRP Research Paper #63
July 1966

The research reported in this paper has been sponsored by the National Aeronautics and Space Administration under grant NASA NsG 333.

PRELIMINARY INVESTIGATION OF PERIPHERAL SUBSIDENCE ASSOCIATED WITH HURRICANE OUTFLOW[1]

Ronald M. Reap

Department of the Geophysical Sciences
The University of Chicago
Chicago, Illinois

ABSTRACT

Synoptic and Nimbus I HRIR data were utilized to determine the vertical temperature, moisture, and cloud distribution within the peripheral divergence area associated with Hurricane Dora. Relationships between the 200 mb shear line, high-level storm outflow, low-level drying and outer convective cloud bands were examined for the period September 8-10, 1964. A zone of low-level cloud suppression, characterized by marked drying and relative warming aloft, was observed 25-100 nautical miles east of the upper shear line. Convective cloud bands were located along the sharp horizontal moisture gradients bordering the zone of pronounced drying. The principle of vertical coupling was proposed as an explanation for the slowly changing structure of temperature, moisture and cloudiness observed relative to the moving 200 mb shear line.

1. Introduction

Evidence of peripheral subsidence has consistently appeared in numerous historical accounts of pre-hurricane divergence. Eyewitness observations recorded 24 to 48 hours prior to the arrival of hurricane conditions have usually indicated the presence of exceptionally clear weather with marked suppression of low-level convective activity and below average amounts of cumuli. Time cross-section analyses of hurricanes Carla and Anna

---

[1]The research reported in this paper has been sponsored by the National Aeronautics and Space Administration under grant NASA NsG 333.

by Fett (1964) have verified the existence of very dry air at the edge of the hurricane circulation. Major cloudiness was found to occur between the dry zones associated with the high-level outflow.

The possibility of a direct hurricane circulation with a subsiding outer branch has been proposed by Riehl (1950), Bergeron (1954) and others. However, such a zone subsidence would act to destroy the initial warm core unless some mechanism was provided to carry away the excess heat. Ventilation of cold mid-tropospheric air was postulated by Riehl (1950) as a possible means of achieving this end.

In examining data from a large number of aircraft reconnaissance flights, Hughes (1952) determined that in the mean all low-level convergence was concentrated within 100 miles of the hurricane center with extreme values at 60 miles. Divergence prevailed beyond a radius of 100 miles at a magnitude comparable to synoptic scale disturbances. However, regions of organized convective activity are frequently observed within the divergence area even though the total amount of low cloudiness may be below average for a tropical or sub-tropical region. Bands of cumulus congestus are often located up to 300 miles from the hurricane center. Evidence presented in the present study indicates a close relationship between the outer convective cloud bands, very dry air, and high-level storm outflow.

Surface, upper-air, and Nimbus I HRIR data obtained from Hurricane Dora of Sept. 1964 were utilized in order to examine the vertical temperature, moisture, and cloud distribution within the peripheral zone of synoptic scale divergence. Dora was observed to move across extreme northern Florida with a major portion of the high-level outflow occuring over the fairly dense upper-air network located in the south-eastern United States. Winds aloft were available every six hours from most reporting stations. Several stations recorded special radiosonde observations every six hours making it possible to analyze the divergence area in great detail.

2. Shear Line Characteristics

The high-level outer shear line may be viewed as the intersection of the hurricane outflow boundary with the 200-mb constant pressure surface. Air within the outflow layer possesses a high equivalent potential temperature relative to air within the adjacent subtropical high. Figure 1 illustrates the westward progression of the shear line as Hurricane Dora slowly approached the Florida coastline. The successive shear line positions were obtained from the reported six-hourly winds aloft. Multiple WRS-57 radar fixes obtained from Daytona Beach, Tampa and Apalachicola were used to plot

the storm track. Radiation data from Nimbus I were analyzed to determine the position of the hurricane eye at 06Z September 9, 1964.

The well-defined northern extent of the shear line was observed to disappear rapidly subsequent to landfall of the hurricane eye at 06Z on September 10. A weakly organized remnant of the shear line was still in existence parallel to the Louisiana Gulf Coast at 12Z on the 10th.

Figure 2 shows the 200 mb contours and shear line position at 00Z September 9. The shear line was located in a trough with strong cyclonic shear evident from the wind field. Increasing contour heights immediately east of the shear line were due to warming below 200 mb resulting from horizontal advection of warm outflow air and sinking due to convergence along the shear line. Decreasing heights farther east of the shear line reflected the rapid decrease in surface pressures toward the hurricane center.

Figure 3 illustrates the high-level warming below 200 mb as recorded by three stations in the vicinity of the shear line. Warming was also observed in the 500 mb to 800 mb layer, a fact discussed later in section 4. As shown by Fig. 3, cooling was observed above the high-level warming. The cooled layer represented negative temperature anomalies which can most logically be explained by the vertical motion field associated with shear line convergence. Positive vertical motion above the level of maximum convergence and sinking below would dynamically produce the observed temperatures. Horizontal advection of warm outflow air offsets to some extent the cooling due to upward vertical motion. A similar temperature structure was observed by Riehl (1954) in his well-documented investigation of a persistent Atlantic shear line.

3. Cloud Distribution Relative to Shear Line

Referring to Fig. 4, we find a bar graph of the mean cloud cover in percent for 14 surface stations as a function of time and distance relative to the 200 mb shear line. Hourly reports of sky cover in tenths over a 24 hour period centered at the shear line passage for each station were used to prepare Fig. 4. The mileage scale was based on an average shear line movement of 12 knots. Positive time and distance values indicate pre-shear line passage. Cloud heights were divided into two catagories: high cloud and low or middle cloud.

We observe from Fig. 4 that the amount of low and middle cloud gradually decreased as the shear line approached. Almost complete suppression of low-level

cloudiness was found 25-100 nautical miles eastward of the shear line. However, a uniform increase in the amount of high-level cirrus and cirrostratus was observed coinciding with the suppression of low and middle clouds. This warm front-like sequence is in complete agreement with observations of pre-hurricane cloudiness recorded in the literature. In addition, note the increase in smoke and haze, an indication of a pronounced inversion which is found in conjunction with the low cloud suppression.

Returning to Figs. 4 and 5, we note that towering cumulus and cumulonimbus were located 100-200 miles either side of the 200 mb shear line position. In order to examine this area of convection in greater detail, a radiation map was prepared from Nimbus I High Resolution Infrared Radiometer (HRIR) data. The Nimbus I radiometer was sensitive in the 3.4 to 4.2 micron near-infrared window. As shown by Fujita and Bandeen (1965), this system provides a significant increase in the quality of mapping detail obtainable from satellite radiation data. Figure 6 gives the radiation pattern for orbit 174 at 0530Z September 9, 1964. The values shown are relative scale values obtained from the original analog traces. Low scale values indicate low temperatures while high scale values represent high temperatures.

Referring to the radiation analysis in Fig. 6, we observe that a banded cloud structure is clearly evident. The band was located approximately 120-130 miles east of the 200 mb shear line which was in good agreement with the surface observations given in Fig. 4. The low-temperature cores within the cloud band corresponded to towering cumulus and cumulonimbus. Increased convective activity was indicated over the Gulf of Mexico where the warm waters provided an ample source of heat and moisture. The somewhat warmer areas surrounding the low-temperature cores represented cirrus and cirrostratus decks associated with these vertical developments. The high temperatures found adjacent to the cloud band corresponded to clear areas where the satellite radiometer recorded radiation from land or sea surfaces.

4. Vertical Temperature and Moisture Distribution

A time cross-section for Valparaiso, Florida covering the period from 00Z on 8 September through 12Z on 12 September is shown in Fig. 7. The shape and location of the outflow boundary was determined from an analysis of the Valparaiso winds in addition to maintaining time and spatial continuity with upper-air winds reported from nearby stations. Figure 8 gives the mixing ratio analysis obtained from the six-hourly

upper-air moisture data for the same period. Note the pronounced drying at 06Z on 9 September, directly below the maximum depth of the high-level outflow. Examination of a similar cross-section for Montgomery, Alabama, not reproduced here, revealed identical drying below the high-level outflow. The minor oscillations represent the diurnal variation of moisture resulting from daytime heating and convection.

Returning again to the 0530Z 9 September, radiation analysis given in Fig. 6, we see that the marked drying in Fig. 8 corresponds to the area labeled "Subsidence Zone." This was also the region of maximum low-cloud suppression located 25-100 nautical miles east of the 200 mb shear line (see Fig. 4). According to Fig. 8, the convective cloud band noted in the radiation analysis was located along the sharp horizontal moisture gradient bordering the subsidence zone. Convective bands are frequently observed to originate along similar moisture gradients. In a study of Hurricane Carla of September 1961, Fett (1964) noted that the passage of the 200 mb outer shear line was followed by an area of organized convection, occasionally of squall line intensity. While investigating the mature and later stages of Hurricane Anna of July 1961, Arnold (1966) also observed a tendency for increased convective activity in the vicinity of the 200 mb shear line.

Figure 9 gives the mixing ratio analysis for Key West, Florida,based on the 00Z and 12Z upper-air data. Marked drying was again observed below the high-level outflow. The diurnal variation of moisture was less pronounced due to the extremely small surrounding land area. Convection in such an oceanic environment would be more dependent on low-level convergence than on daytime heating over land.

A series of upper-air moisture profiles for Miami, Key West, and Valparaiso are shown in Fig. 10. The soundings were grouped according to station distance from the 200 mb outer shear line with negative values representing distance east and positive values as distance west. It is interesting to note the similarity of the moisture profiles when related to the shear line. Examining group A, we note the initial influx of dry air some 100-150 miles west of the shear line. A progressive lowering of the dry layer base and temperature inversion was indicated by group B. Group C showed marked drying below 900 mb up to 100 miles east of the shear line. Group D reflected the gradual increase in moisture toward the approaching hurricane.

In order to examine further the synoptic scale divergence area, several space cross-sections were prepared along two axes oriented toward the hurricane center. The mixing ratio cross-section for 00Z September 9, (Fig. 11) extended northeast from

Grand Cayman (383) to Key West, Miami and Grand Bahama (063). The boundary of the high-level outflow was determined from continuity and all available winds aloft data. Marked drying was again present below the high-level outflow. The low moisture value of 0.6 gm/kg at 450 mb was obtained from continuity. The increase in moisture at Grand Bahama was recorded 180 miles southwest of the hurricane center. Note that the motion of the maximum drying phase over Miami and Key West, as given in Figs. 10-11, closely corresponds to the 12 kt shear line movement. The approximate times of greatest drying aloft at Miami and Key West were, respectively, 18Z September 8, and 06Z September 9.

The mixing ratio cross-section for 12Z September 9, shown in Fig. 12, extends west to east from Lake Charles through Burrwood, and Valparaiso to Jacksonville. Drying below the high-level outflow was even more pronounced than that observed at Key West in Fig. 11. The expected increase in moisture 130 miles west of the hurricane center was reflected in the Jacksonville sounding.

Figure 13 shows the cross-section of potential temperature corresponding to the mixing ratio analysis given in Fig. 11. In agreement with Fig. 3, a steepening of the high-level lapse rate was observed due to convergence along the 200 mb shear line. Low-level warming was also observed with the potential temperatures between 500 mb and 800 mb decreasing toward Grand Bahama. The warming below 500 mb indicated in Fig. 3 and Fig. 13 was clearly shown by a temperature anomaly cross-section prepared for Valparaiso. Figure 14 shows that the 700 mb to 800 mb layer was warmed by approximately 5°C in conjunction with marked low-level drying. Cooling was observed for some distance east of the dry region toward the hurricane circulation.

Contours and isotherms at the 750 mb surface for 00Z September 9 are shown in Fig. 15. The axis of highest temperature was located immediately east of the 200 mb shear line. An identical relationship was shown by the 750 mb analysis for 12Z September 8, not reproduced herein. Examining the 750 mb analysis for 12Z September, given in Fig. 16, we observe that the warm tongue was again located in the same position relative to the 200 mb shear line. The lower temperatures east of the warm tongue were associated with a cool rain area located at the outer fringes of the main hurricane circulation.

At this point we must consider the contribution of horizontal advection to the establishment of the tongue of warm dry air observed on the 750 mb charts. The over-water trajectory of air entering the southeastern U.S., as given in Figs. 15 and 16, does not indicate a source for the very dry air. From the air mass concept we would

expect the surface conditions to reflect a change of air mass if the drying were due solely to horizontal advection. However, referring to Figs. 8-14, we note that characteristically of tropical regions the amplitude of temperature and moisture changes increased upward. Horizontal advection of dry air between 700 mb and 900 mb was indicated by Group A in Fig. 10 and by Fig. 12. The source region for this horizontally advected dry air appeared to be the more slowly moving zone of pronounced low-level drying east of the 200 mb shear line.

5. Summary and Conclusions

A zone of low-level cloud suppression, characterized by marked drying and relative warming aloft, was located below the maximum depth of the high-level hurricane outflow. The zone extended from 25-100 nautical miles east of the 200 mb shear line and was observed to maintain the same relative position over a 48 hour period. Moisture profiles from widely scattered upper-air stations appeared very similar when related to passage of the upper shear line. As shown in the Nimbus I HRIR and synoptic analyses, convective cloud bands were located below an area of divergence at 200 mb and along the sharp horizontal moisture gradients bordering the zone of pronounced drying. Since the moisture and temperature structure did not vary significantly with time relative to the moving 200 mb shear line, we may conclude that dynamic features of the wind field aloft governed the observed gradients of moisture and temperature and subsequent formation of the convective cloud bands.

A possible explanation for the close relationship between the high-level hurricane outflow and low-level drying lies in the principle of vertical coupling. In daily tropical situations an existing upper shear line is usually accompanied by a diverging and subsiding current at some lower level. Convergence tends to steepen the lapse rate in the high troposphere, as noted in the present study, while divergence stabilizes it in the lower levels, except for the mixed layer near the ground. The low-level subsiding current was indicated by the relative warming and sharp decrease in moisture observed subsequent to shear line passage.

Acknowledgements: The author is very grateful to Dr. Tetsuya Fujita for his many valuable suggestions and comments. Gratitude is also expressed to Mr. William Winkler for his assistance in compiling and plotting various data.

REFERENCES

Arnold, J., 1966: The time change of cloud and circulation features in Hurricane Anna 1961 from easterly wave stage to dissipation. SMRP Research Paper No. 64, Univ. of Chicago.

Bergeron, T., 1964: The problems of tropical hurricanes. Quart. J. R. Meteor. Soc., 80, 131-164.

Fett, R., 1964: Aspects of hurricane structure: new model considerations suggested by TIROS and Project Mercury observations. Mon. Wea. Rev., 92, 43-60.

Fujita, T. and W. Bandeen, 1965: Resolution of the Nimbus high resolution infrared radiometer. SMRP Research Paper No. 40, Univ. of Chicago, 11 pp.

Hughes, L., 1952: On the low-level wind structure of tropical storms. J. Meteor., 9, 422-428.

Riehl, H., 1954: Tropical Meteorology, McGraw-Hill Co., New York, 243-249.

_____, 1950: A model of hurricane formation. J. Appl. Physics, 21, 917-925.

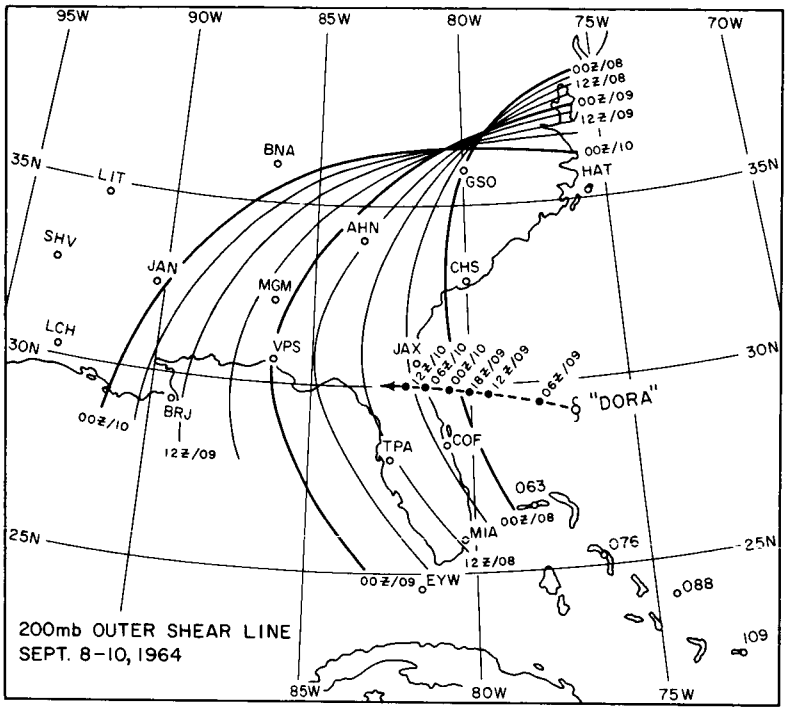

Fig. 1. Six-hourly positions of the 200 mb outer shear line for Hurricane Dora during the period September 8-10, 1964.

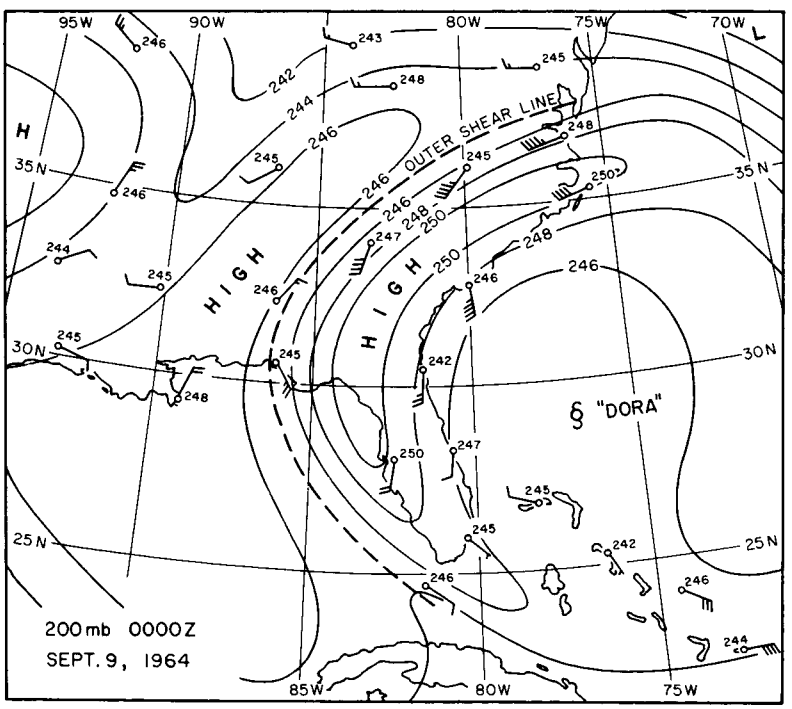

Fig. 2. 200 mb contour map (20 m intervals) and shear line position for 00Z September 9, 1964.

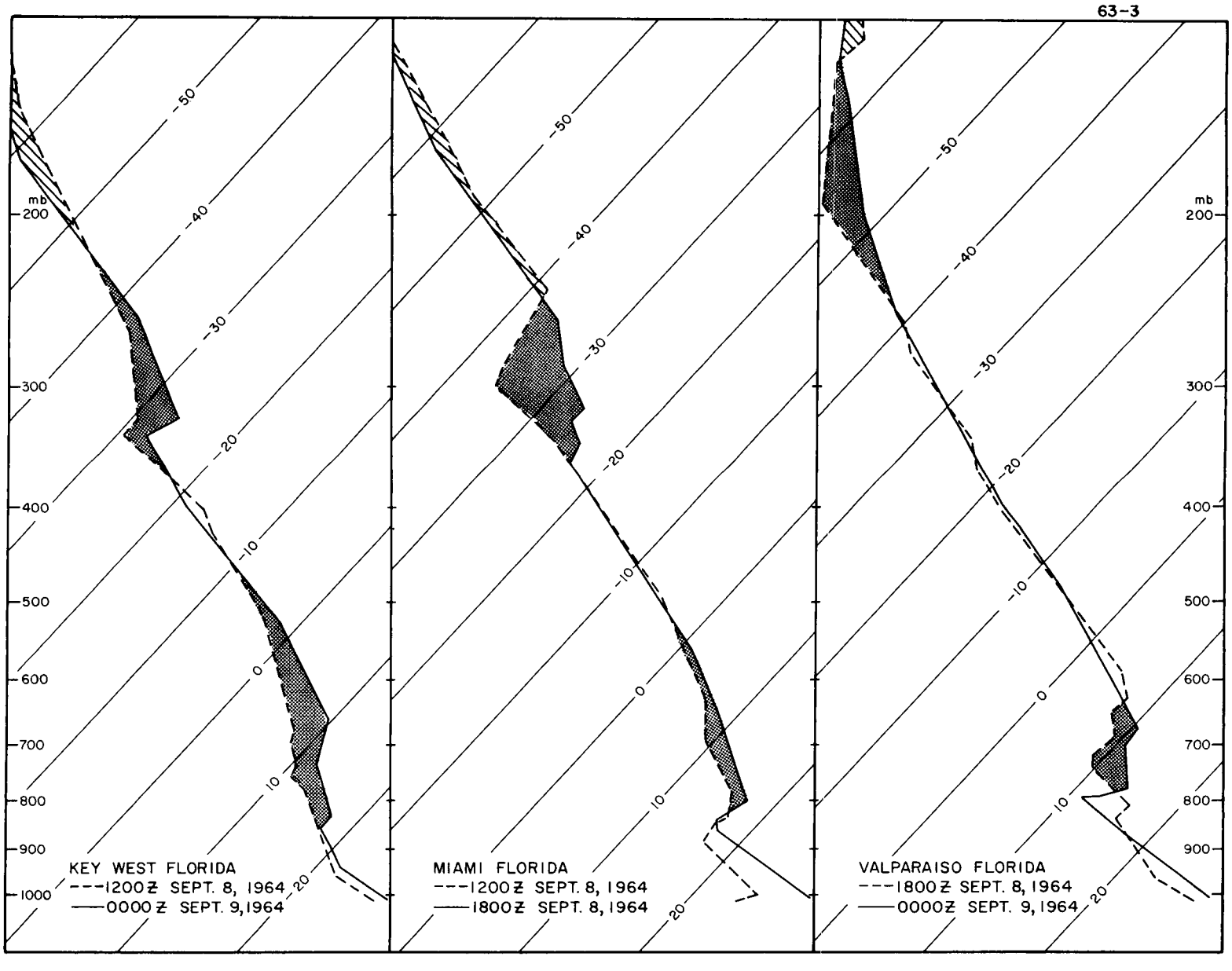

Fig. 3. Upper-air soundings from three stations in the vicinity of the 200 mb shear line. Note the high-level warming and cooling due to convergence along the upper shear line. The warming below 500 mb was observed in conjunction with marked low-level drying.

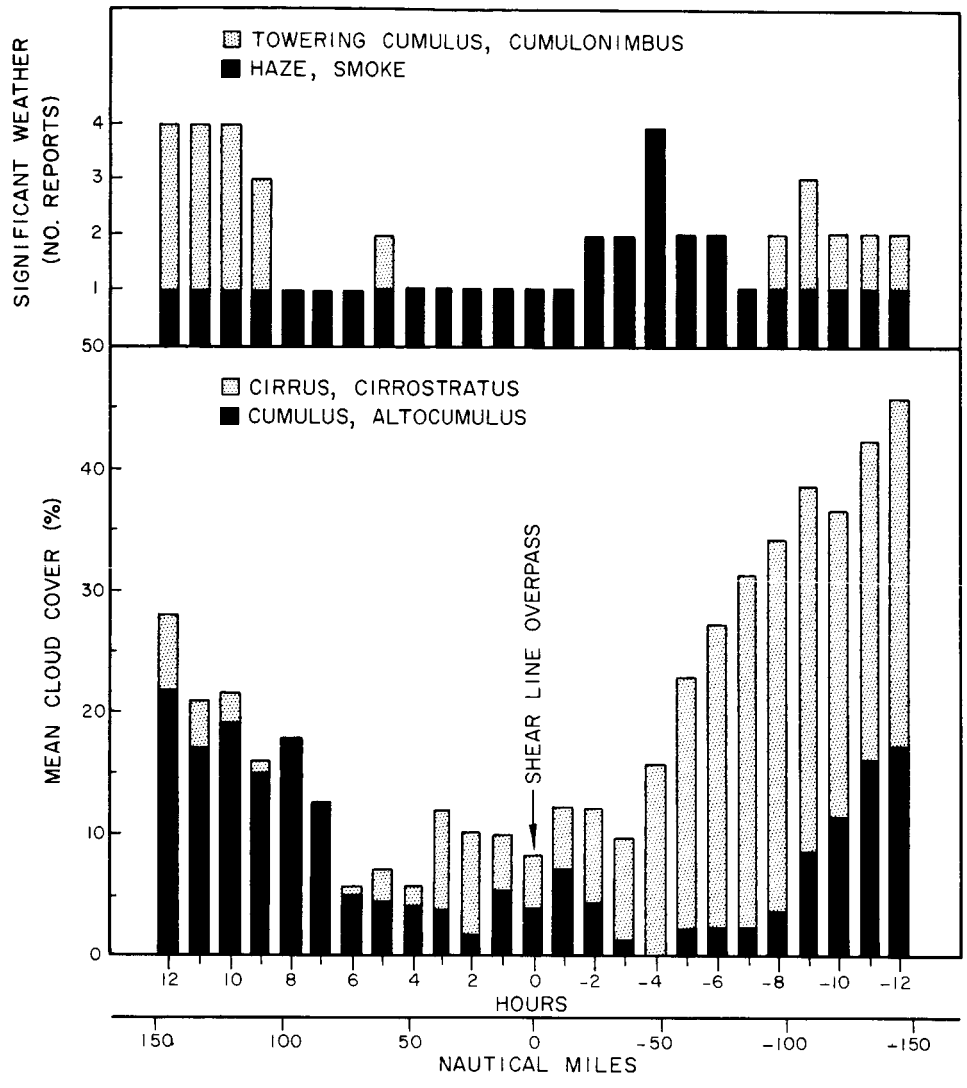

Fig. 4. Bar graph of the mean cloud cover for 14 first order surface stations as a function of time and distance relative to the 200 mb shear line. Positive time and distance values indicate pre-shear line passage. Note the post-shear line suppression of low-level cloudiness and convection.

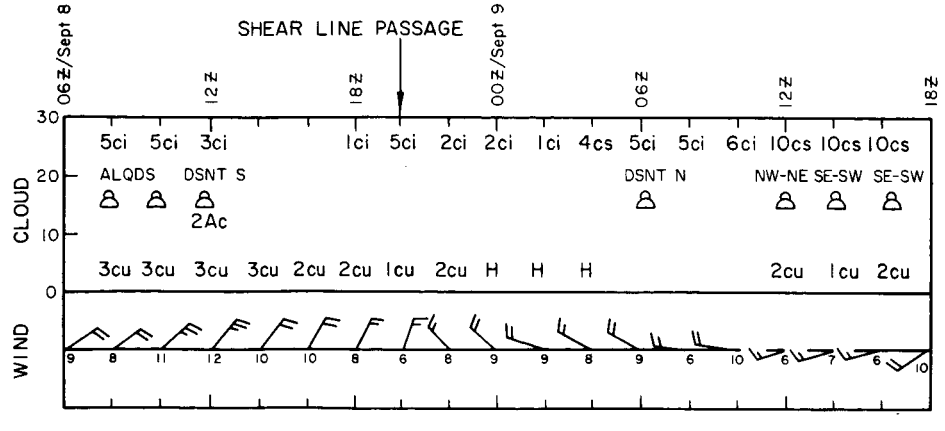

Fig. 5. Surface observations recorded at Key West, Fla. indicating low-level cloud suppression and areas of convection 100-200 naut. miles either side of the 200 mb shear line position.

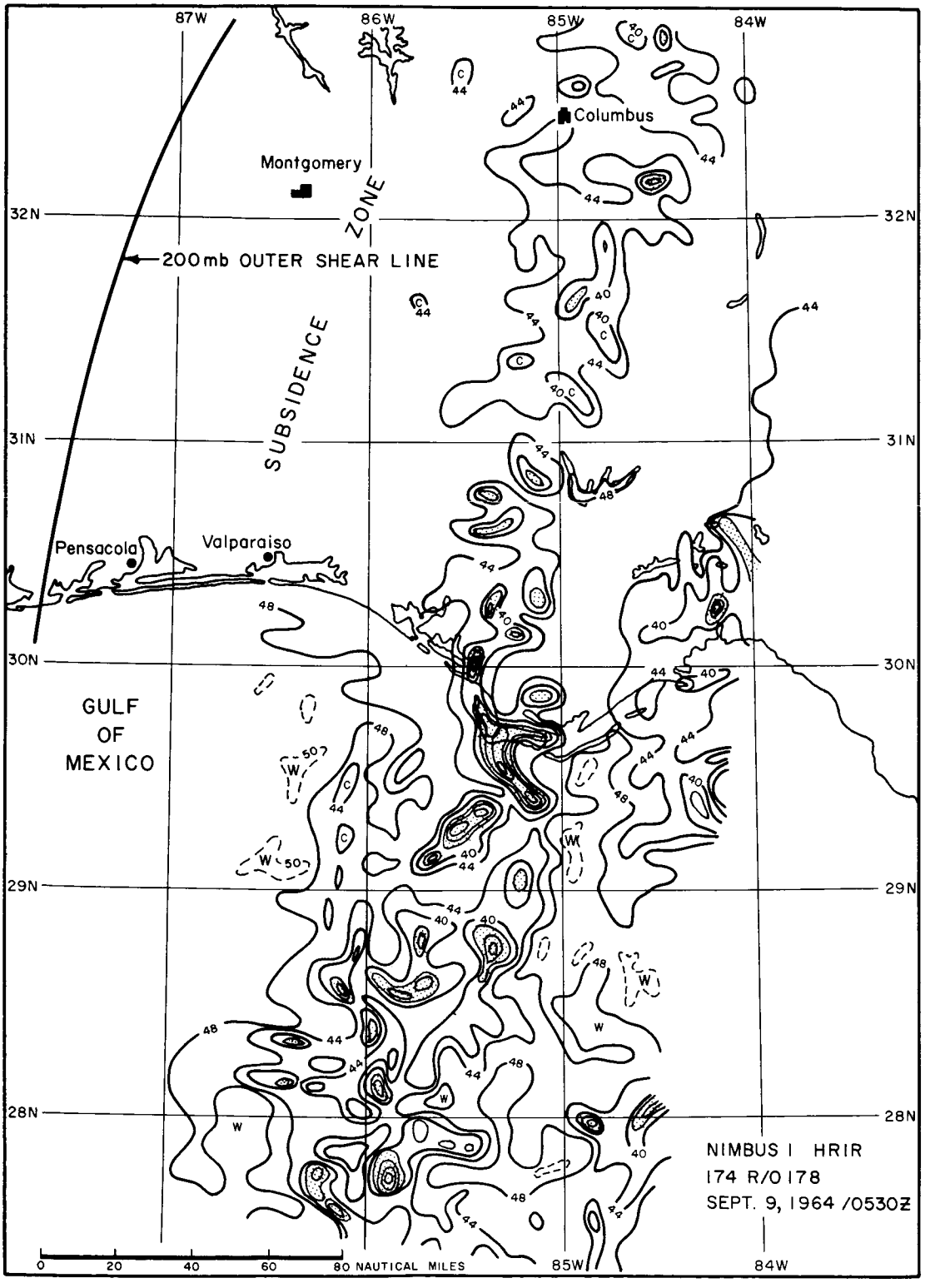

Fig. 6. Relative scale values of radiation obtained from the original Nimbus I analog traces for Orbit 174, September 9, 1964. Low scale values represent vertical cloud developments while high scale values indicate clear areas or scattered or thin cloudiness. The subsidence zone corresponds to the region of maximum cloud suppression located 25-100 naut. miles east of the 200 mb shear line.

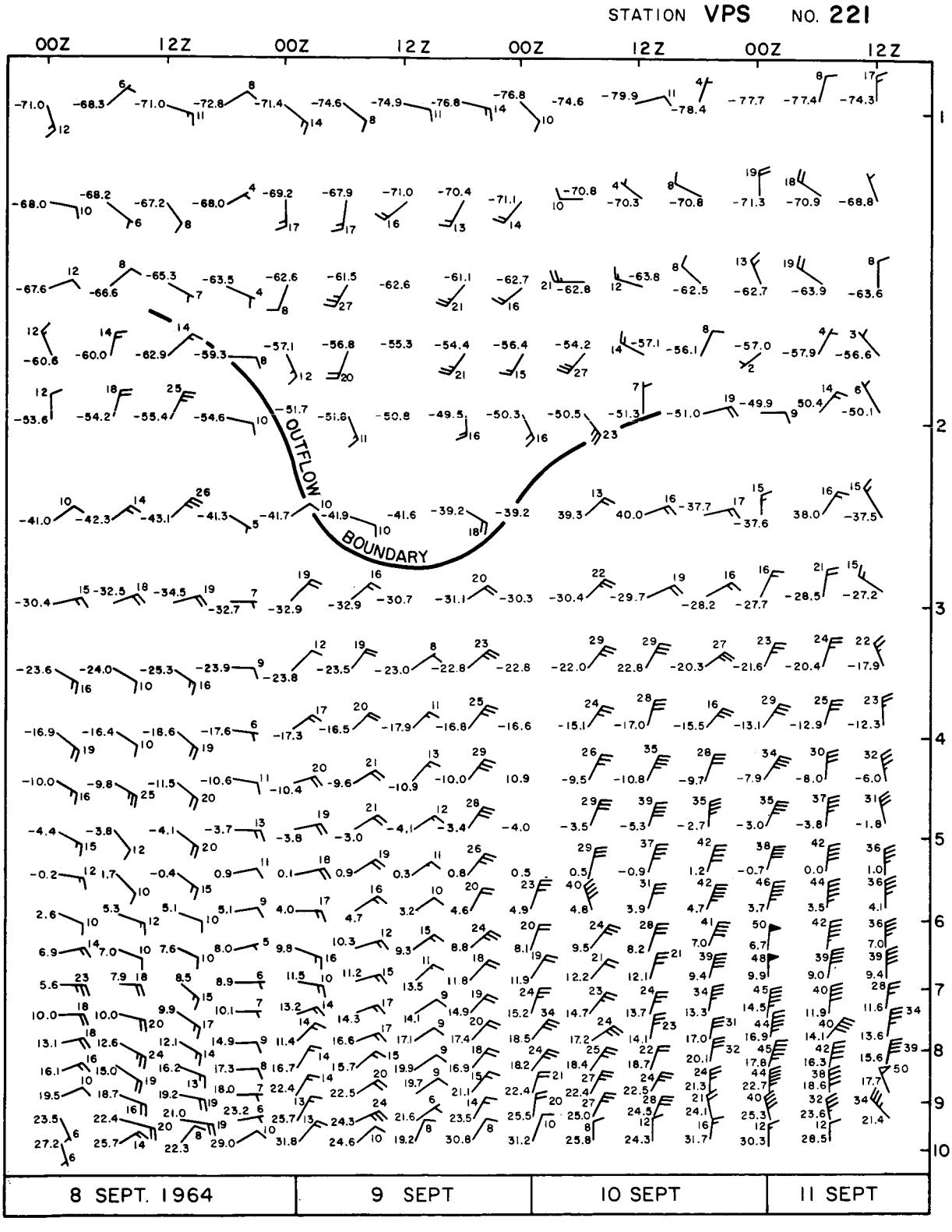

Fig. 7. Upper-air temperatures and winds and hurricane outflow boundary for Valparaiso, Fla. during the period September 8-11, 1964.

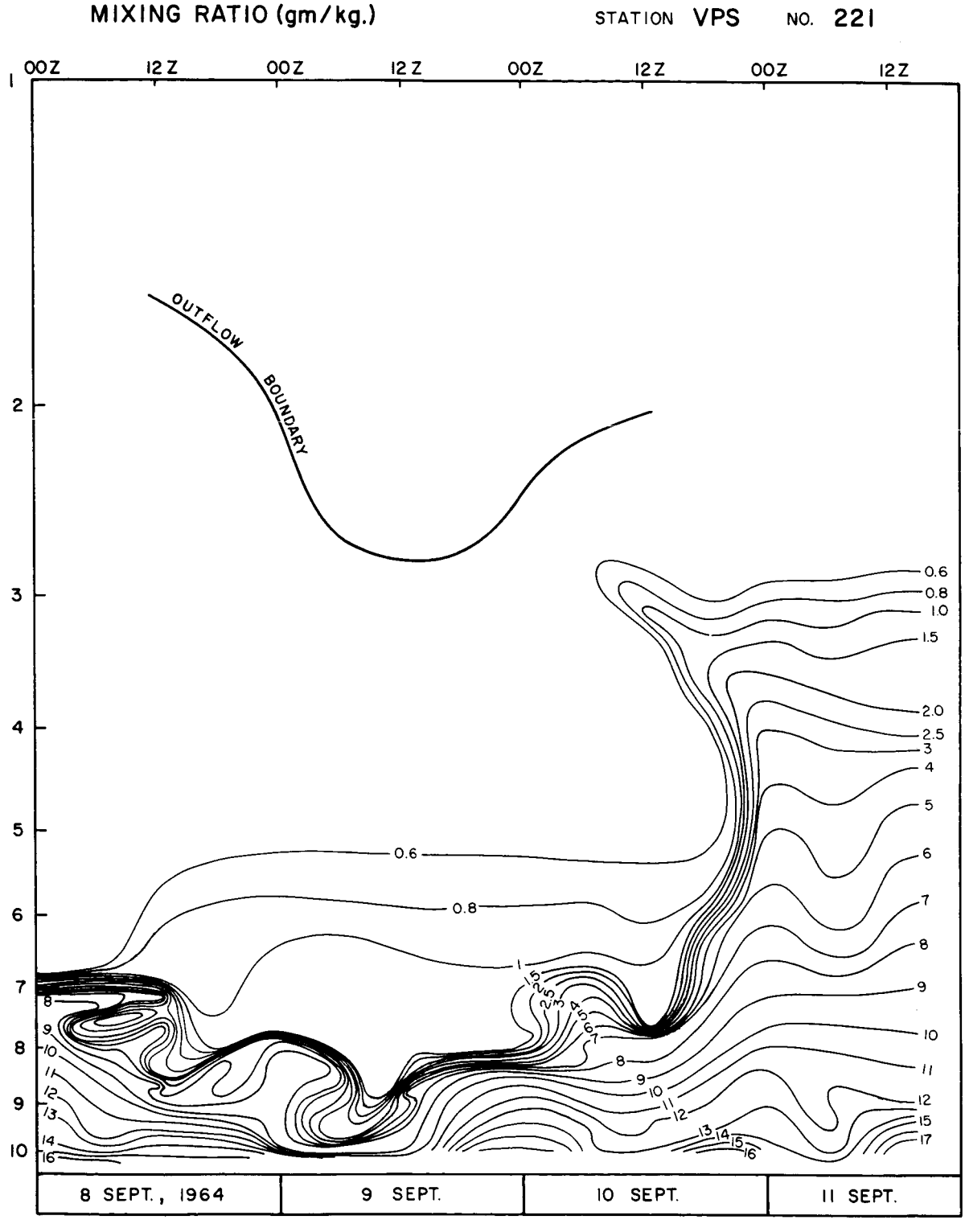

Fig. 8. Mixing ratio analysis (gm/kg) and outflow boundary obtained from six-hourly upper-air soundings for Valparaiso, Fla.

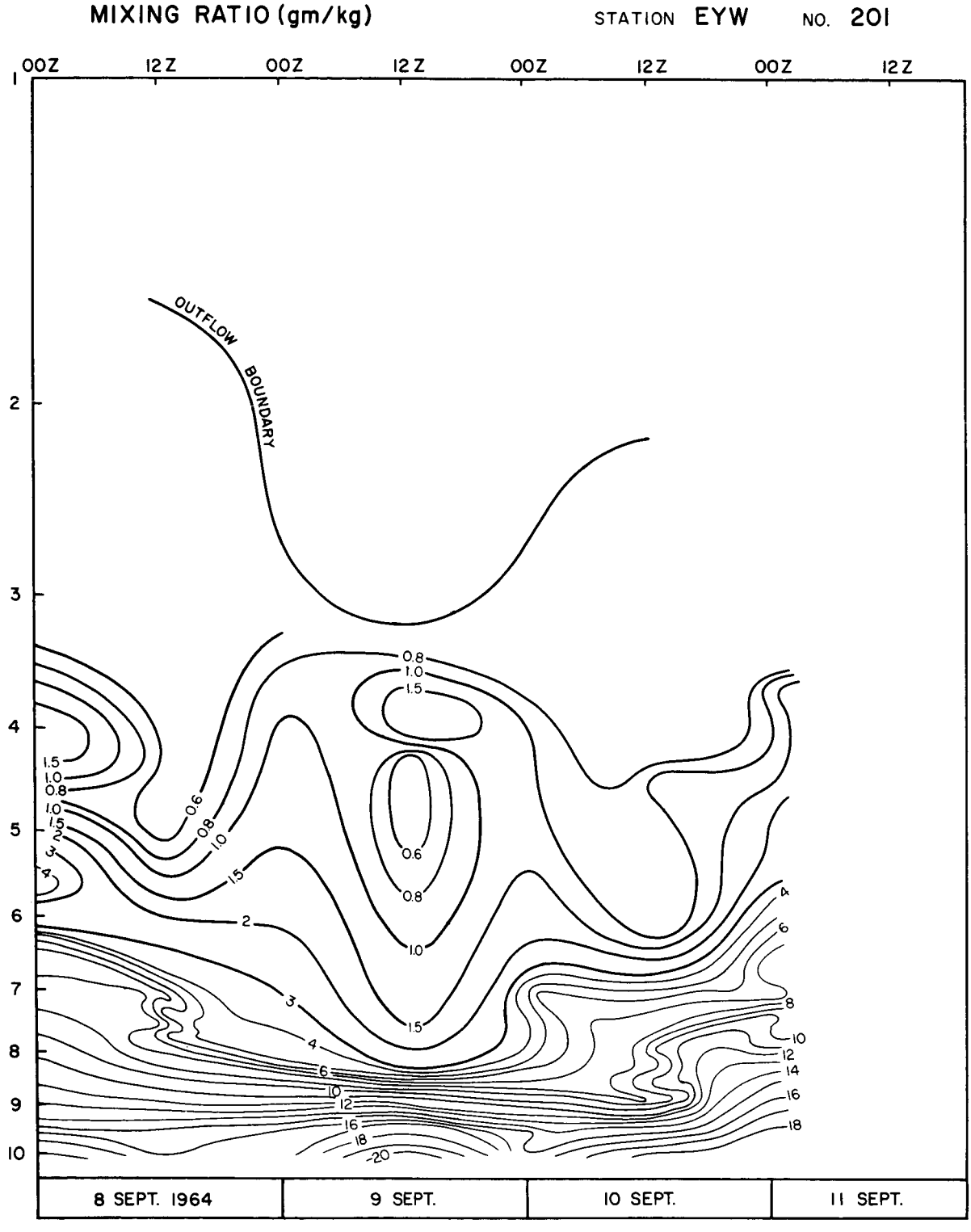

Fig. 9. Mixing ratio analysis (gm/kg) and outflow boundary obtained from 00Z and 12Z upper-air data for Key West, Fla.

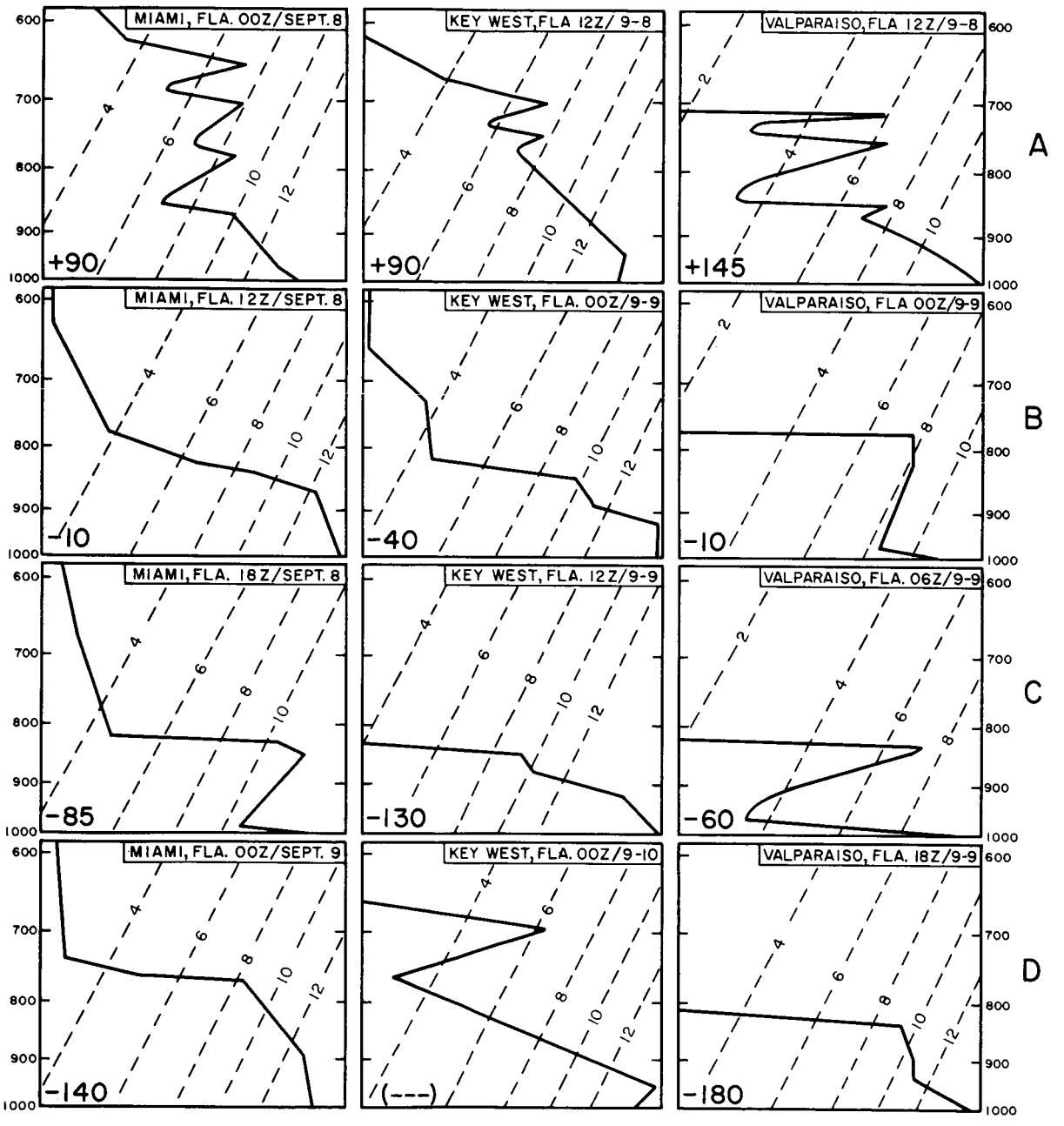

Fig. 10. Upper-air moisture profiles (gm/kg) for Miami, Key West, and Valparaiso, Fla. grouped according to station distance from the 200 mb shear line. Mileage east (negative) or west (positive) relative to the shear line is indicated in the lower left of each diagram.

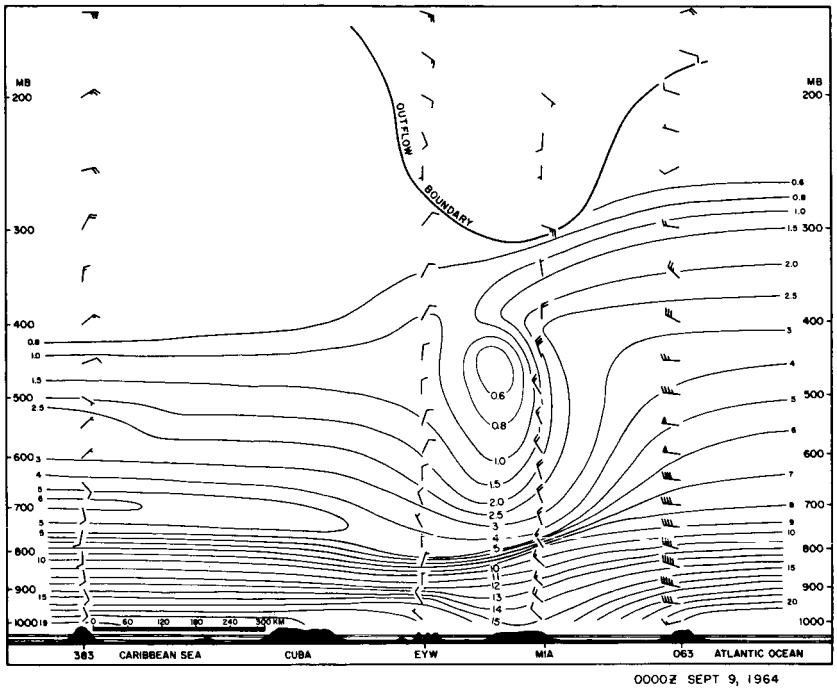

Fig. 11. Mixing ratio (gm/kg) cross section for 00Z September 9, 1964 extending northeast from Grand Cayman (383) to Key West, Miami and Grand Bahama (063). Hurricane Dora was located 180 naut. miles northeast of Grand Bahama. Note the pronounced drying below the maximum depth of the high-level outflow.

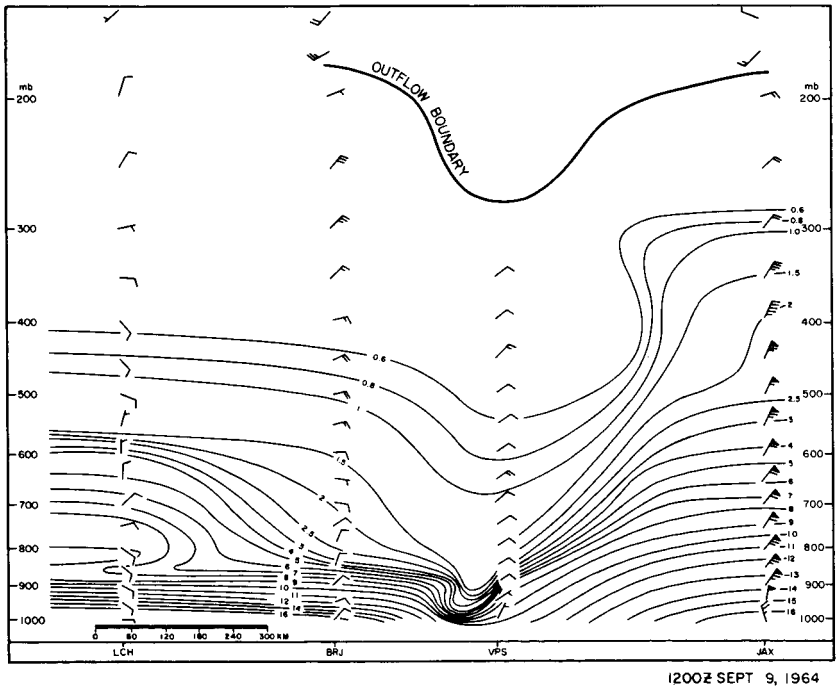

Fig. 12. Mixing ratio (gm/kg) cross-section for 12Z September 9, 1964 extending west to east from Lake Charles through to Burrwood, and Valparaiso to Jacksonville. Hurricane Dora was located 130 east of Jacksonville.

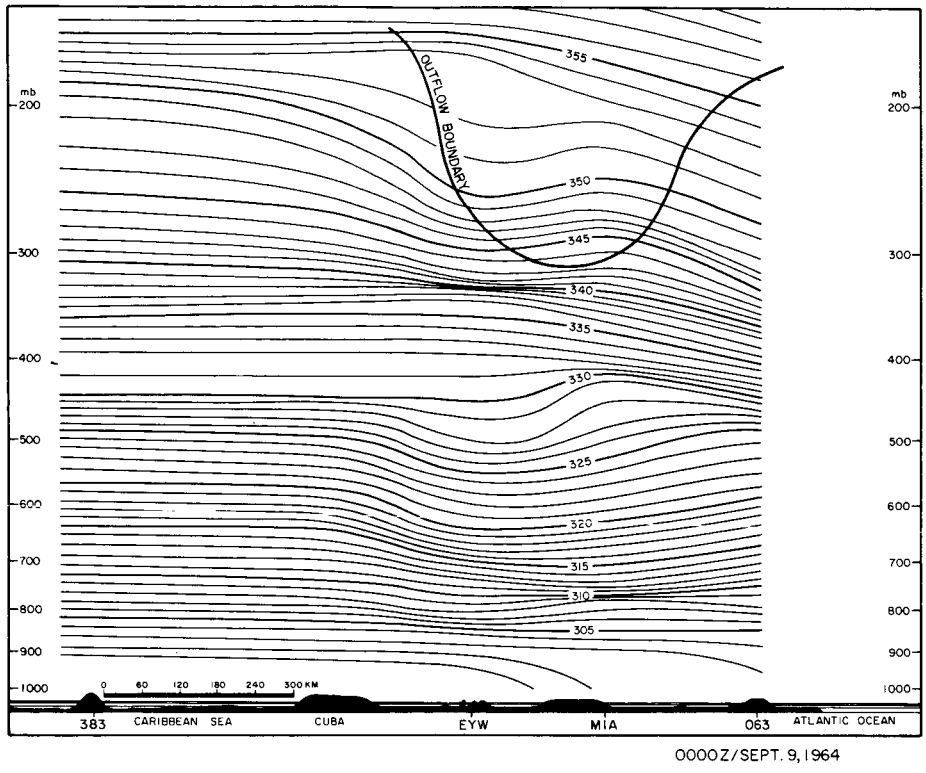

Fig. 13. Potential temperature cross-section for 00Z September 9, 1964 extending northeast from Grand Cayman (383) to Key West, Miami and Grand Bahama (063). A steepening of the high-level lapse rate was observed due to convergence along the upper shear line.

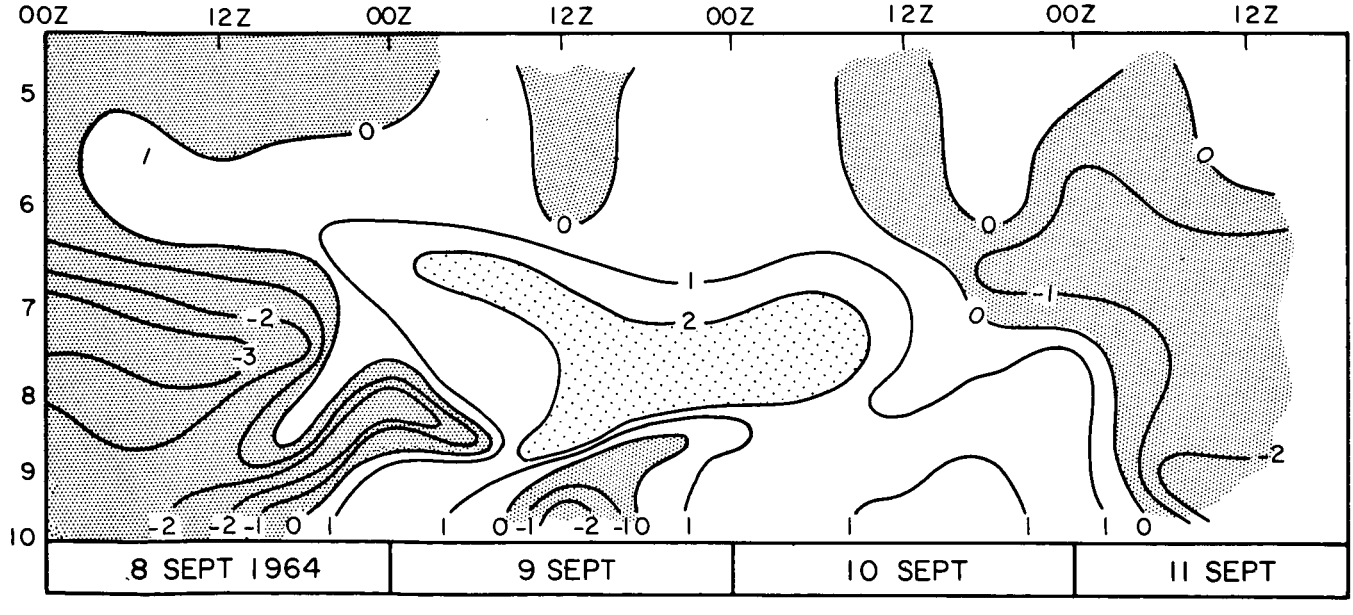

Fig. 14. Upper-air temperature anomalies for Valparaiso, Fla. during the period September 8-11, 1964. The warming below 500 mb was observed in conjunction with marked low-level drying.

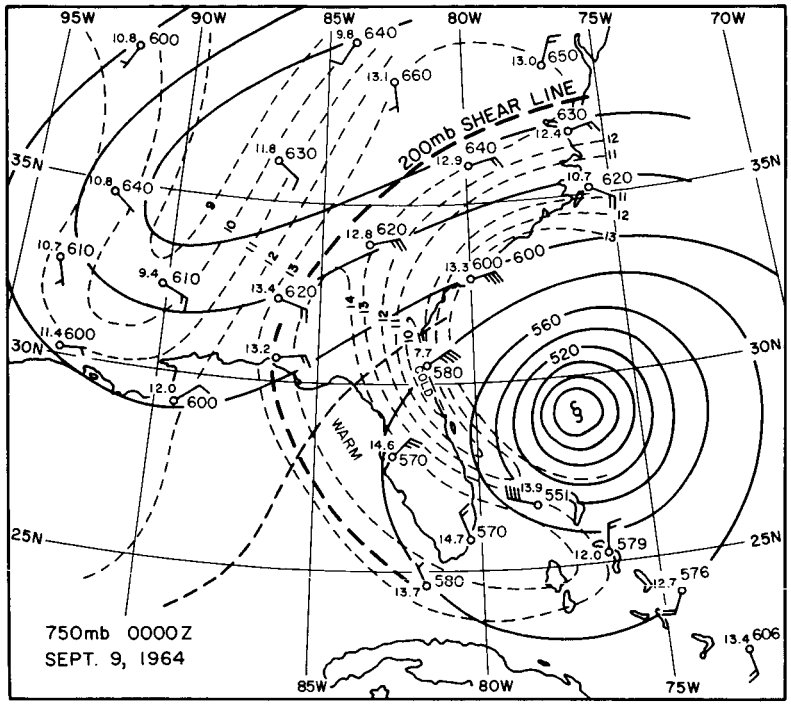

Fig. 15. 750 mb chart with contours (20 m intervals), isotherms (°C), line position for 00Z September 9, 1964. Note the warm tongue located east of the upper shear line.

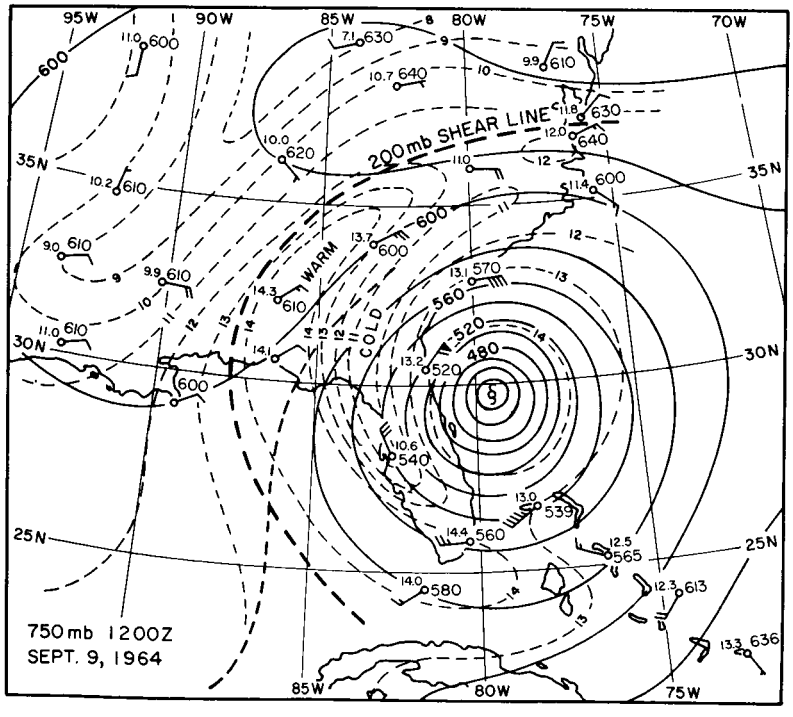

Fig. 16. 750 mb chart with contours (20 m intervals), isotherms (°C), and shear line position for 12Z September 9, 1964. The warm tongue located east of the upper shear line maintained the same relative position over a 48 hour period.

MESOMETEOROLOGY PROJECT - - - RESEARCH PAPERS

(Continued from front cover)

42. A Study of Factors Contributing to Dissipation of Energy in a Developing Cumulonimbus - Rodger A. Brown and Tetsuya Fujita
43. A Program for Computer Gridding of Satellite Photographs for Mesoscale Research - William D. Bonner
44. Comparison of Grassland Surface Temperatures Measured by TIROS VII and Airborne Radiometers under Clear Sky and Cirriform Cloud Conditions - Ronald M. Reap
45. Death Valley Temperature Analysis Utilizing Nimbus I Infrared Data and Ground-Based Measurements - Ronald M. Reap and Tetsuya Fujita
46. On the "Thunderstorm-High Controversy" - Rodger A. Brown
47. Application of Precise Fujita Method on Nimbus I Photo Gridding - Lt. Cmd. Ruben Nasta
48. A Proposed Method of Estimating Cloud-top Temperature, Cloud Cover, and Emissivity and Whiteness of Clouds from Short- and Long-wave Radiation Data Obtained by TIROS Scanning Radiometers - T. Fujita and H. Grandoso
49. Aerial Survey of the Palm Sunday Tornadoes of April 11, 1965 - Tetsuya Fujita
50. Early Stage of Tornado Development as Revealed by Satellite Photographs - Tetsuya Fujita
51. Features and Motions of Radar Echoes on Palm Sunday, 1965 - D. L. Bradbury and Tetsuya Fujita
52. Stability and Differential Advection Associated with Tornado Development - Tetsuya Fujita and Dorothy L. Bradbury
53. Estimated Wind Speeds of the Palm Sunday Tornadoes - Tetsuya Fujita
54. On the Determination of Exchange Coefficients: Part II - Rotating and Nonrotating Convective Currents - Rodger A. Brown
55. Satellite Meteorological Study of Evaporation and Cloud Formation over the Western Pacific under the Influence of the Winter Monsoon - K. Tsuchiya and T. Fujita
56. A Proposed Mechanism of Snowstorm Mesojet over Japan under the Influence of the Winter Monsoon - T. Fujita and K. Tsuchiya
57. Some Effects of Lake Michigan upon Squall Lines and Summertime Convection - Walter A. Lyons
58. Angular Dependence of Reflection from Stratiform Clouds as Measured by TIROS IV Scanning Radiometers - A. Rabbe
59. Use of Wet-beam Doppler Winds in the Determination of the Vertical Velocity of Raindrops inside Hurricane Rainbands - T. Fujita, P. Black and A. Loesch
60. A Model of Typhoons Accompanied by Inner and Outer Rainbands - Tetsuya Fujita, Tatsuo Izawa, Kazuo Watanabe, and Ichiro Imai

MESOMETEOROLOGY PROJECT - - - RESEARCH PAPERS

(Continued from inside back cover)

61. Three-Dimensional Growth Characteristics of an Orographic Thunderstorm System - Rodger A. Brown.

62. Split of a Thunderstorm into Anticyclonic and Cyclonic Storms and their Motion as Determined from Numerical Model Experiments - Tetsuya Fujita and Hector Grandoso.